


Performance Enhancement of Photovoltaic Water Pumping System Based on BLDC Motor under Partial Shading Condition [†]

Abdelkarim Ammar ^{1,*} , Kahina Hamraoui ², Moufida Belguellaoui ² and Aissa Kheldoun ¹

¹ Signals and Systems Laboratory LSS, Institute of Electrical and Electronic Engineering, University of M'hamed BOUGARA of Boumerdes, Boumerdes 35000, Algeria; aissa73@gmail.com

² Power and Control Engineering Department, Institute of Electrical and Electronic Engineering, University of M'hamed BOUGARA of Boumerdes, Boumerdes 35000, Algeria; hamraouikahina7@gmail.com (K.H.); beluellaoui.moufida@gmail.com (M.B.)

* Correspondence: a.ammar@univ-boumerdes.dz

[†] Presented at the 1st International Conference on Computational Engineering and Intelligent Systems, Online, 10–12 December 2021.

Abstract: The use of photovoltaic (PV) energy for water pumping is considered one of the most promising areas of photovoltaic applications. This work aims to improve the power extraction of a battery-less photovoltaic pumping system. The DC–DC converter is used to accomplish the maximum power point tracking (MPPT). In addition, the BLDC motor is used for maximum exploitation of the delivered power by the PV array, and to enhance the reliability of the pumping system. Furthermore, an MPPT strategy, based on the cuckoo swarm optimization technique, has been developed to improve the control performance under partial shading conditions. The effectiveness of the proposed system has been examined through simulation using MATLAB and Simulink software.

Keywords: photovoltaic (PV); solar water pumping system (SWPS); maximum power point tracking (MPPT); brushless direct current (BLDC) motor; partial shading; cuckoo search (CS)



Citation: Ammar, A.; Hamraoui, K.; Belguellaoui, M.; Kheldoun, A. Performance Enhancement of Photovoltaic Water Pumping System Based on BLDC Motor under Partial Shading Condition. *Eng. Proc.* **2022**, *14*, 22. <https://doi.org/10.3390/engproc2022014022>

Academic Editors: Abdelmadjid Recioui, Hamid Bentarzi and Fatma Zohra Dekhandji

Published: 15 February 2022

Publisher's Note: MDPI stays neutral with regard to jurisdictional claims in published maps and institutional affiliations.



Copyright: © 2022 by the authors. Licensee MDPI, Basel, Switzerland. This article is an open access article distributed under the terms and conditions of the Creative Commons Attribution (CC BY) license (<https://creativecommons.org/licenses/by/4.0/>).

1. Introduction

Water resources are essential for satisfying human needs, ensuring food production and protecting health, as well as for social and economic development. Worldwide, water pumping is generally dependent on electricity or diesel-generated electricity. Diesel is expensive and scarce in the countryside of many developing countries, and even when it is available, transporting it to remote areas is difficult. This is because there are no roads or supporting infrastructure in most of the remote villages. In rural areas, the installation of a new transmission line and transformers is extremely expensive for irrigation or drinking water [1]. A solar water pumping system (SWPS) is made up of various components that can be classified as mechanical, electrical, or electronic. These components have different construction, operation, and performance characteristics [2].

PV pumping systems based on AC motors, especially induction motors (IM), are often favored because they are more dependable, cost less, and do not need regular maintenance. DC motors are commonly used in low-power solar PV water pumps [3]. However, DC motors with brushes possess low efficiency, and they need frequent maintenance, owing to the sliding brush contacts and the commutator. Three-phase brushless direct-current (BLDC) motors are suitable options, due to their high-efficiency capabilities, compactness, and easy-to-drive qualities [4]. Therefore, this motor has gained considerable attention for water pumping in the recent decade, due to its many advantages, which constitute its desirable characteristics, especially for this application [3].

The use of maximum power point tracking (MPPT) methods is critical to increase the efficiency of photovoltaic (PV) systems. Because of its good balance between complexity, precision, and dependability, the perturb and observe (P&O) approach is the most

prevalent algorithm [5]. It does, however, have several disadvantages, such as a delayed response time, steady-state power oscillation around the MPP, and poor tracking under abrupt irradiance changes or shading effects [6]. Particle swarm optimization (PSO) and cuckoo search (CS) are two optimization strategies that have been proposed to increase the performance of MPPT [7]. Cuckoo search (CS) is an evolutionary optimization technique that was inspired by a type of bird, named the cuckoo [8], by Yang and Deb (2009). Cuckoos put their eggs in other birds' or species' nests [9]. They fly from one nest to the next, looking for the best one, the one that offers the greatest possibility of the eggs hatching successfully. Several papers [10,11] have discussed the applicability of CS to MPPT. It is shown that it is more stable, has greater convergence, and is more efficient.

In this paper, we present a method for tracking the maximum power point of solar water pumping systems under partial shading conditions. The proposed system is based on a BLDC motor to improve the reliability and efficiency of the system. Moreover, a cuckoo search algorithm is proposed to overcome the disadvantages of the conventional MPPT algorithm. The proposed system has been investigated using MATLAB/Simulink software.

2. Configuration of the PV Pumping System

Figure 1 depicts the designed solar water pumping system's configuration. The photovoltaic generator (PVG) is a group of solar panels with connections that are selected to meet the power needs of the association's power electronic converters, motor, and centrifugal pump. The DC–DC converter is connected between a PVG and a pump to extract the maximum energy possible throughout the day. The peak power operating point of the PVG is tracked using an MPPT algorithm, under various conditions [12].

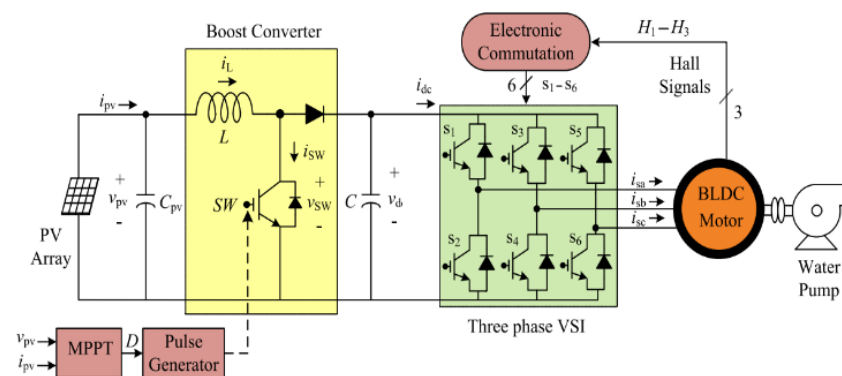


Figure 1. Configuration of the solar PV boost converter BLDC motor-driven water pump.

To control the BLDC motor, a voltage source inverter must be included, which provides three-phase voltages. The boost duty cycle is obtained by the MPPT algorithm, which mainly depends on irradiance.

2.1. Photovoltaic Module

For simplicity and accuracy, the single-diode model is the most studied and used in this work. The single-diode model is shown in Figure 2, and includes a photo current source, a parallel diode, and series and shunt resistors, R_s and R_{sh} , respectively [13].

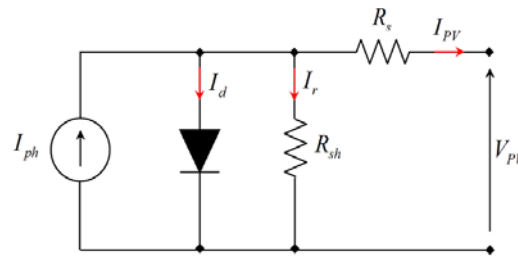


Figure 2. The equivalent circuit of a PV cell.

The model in Figure 2 can be mathematically described by the following equation:

$$I_{PV} = I_{ph} - I_d - I_r = I_{ph} - I_o \left(e^{\frac{V_{PV} + R_s I_{PV}}{n V_t}} - 1 \right) - \frac{V_{PV} + R_s I_{PV}}{R_{sh}} \quad (1)$$

where V_t is the thermal voltage, given by the following:

$$V_t = \frac{k T}{q} \quad (2)$$

k is the Boltzmann constant (1.38×10^{-23} J/K), T is the absolute temperature (k), and q is the electronic charge (1.6×10^{-19} C).

The PV array output current and voltage can be computed according to the parallel- and series-connected modules. The PV module considered in this work is the TSM-250PA05.08 PV module, Trinasolar, China.

2.2. DC–DC Boost Converter

The step-up chopper can be applied to MPPT systems in which the output voltage needs to be greater than the input voltage. The relation between the output and input voltages (V_{out} and V_{in} , respectively) is as follows:

$$\frac{V_{out}}{V_{in}} = \frac{1}{1 - D} \quad (3)$$

where D is the duty cycle; the duty cycle always ranges from zero to one.

2.3. Brushless DC Motor

The BLDC motor’s mathematical model can be formed in the same way as a three-phase synchronous machine. Similarly, with the BLDC motor, the armature winding model is stated as follows [14]:

$$\begin{cases} V_a = R i_a + L \frac{di_a}{dt} + e_a \\ V_b = R i_b + L \frac{di_b}{dt} + e_b \\ V_c = R i_c + L \frac{di_c}{dt} + e_c \end{cases} \quad (4)$$

2.4. Centrifugal Pump

A centrifugal pump is a mechanical device that uses centrifugal force to transfer mechanical energy into pressure in a fluid. Its efficiency is rather good, and it can pump a huge amount of water [1]. The pump’s torque is proportional to the rotor’s squared speed, as follows:

$$T_L = K_P \Omega_r^2 \quad (5)$$

where K_P is the proportionality constant, and it is given by the following:

$$K_p = P_{np} / \Omega_{rn}^3 \quad (6)$$

The pump’s head and available mechanical power at the rotating impeller determine the pump’s water flow and pressure. Affinity laws, which only require the pump ratings and actual input parameters, rotor speed and torque [1], might simplify the estimation of the pump’s output characteristics.

$$\begin{cases} H' = (\Omega_r / \Omega_{rn})^2 \cdot H \\ Q' = (\Omega_r / \Omega_{rn}) \cdot Q \\ P' = (\Omega_r / \Omega_{rn})^3 \cdot P \end{cases} \quad (7)$$

where H , Q and P are the rated parameters of the pump at the rated speed, and Ω_{rn} , H' , Q' and P' are the parameters of the pump at speed Ω_r , which is different to the rated speed.

3. Solar Water Pumping System Control

3.1. Maximum Power Point Tracking

The perturb and observe (P&O) method is a basic iterative approach. It perturbs the operational point of the system, causing the PV array terminal voltage to oscillate about the MPP voltage, even though the solar irradiation and the cell temperature are constant. Figure 3 depicts the P&O algorithm flowchart [15].

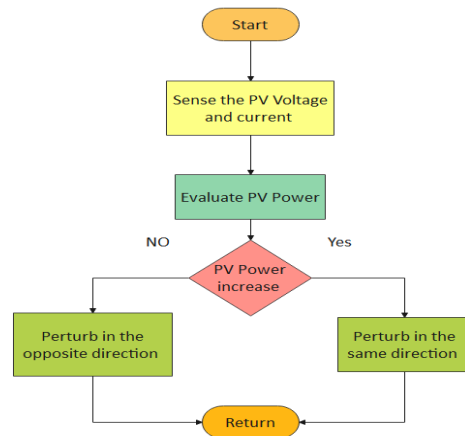


Figure 3. Flowchart of P&O algorithm.

3.2. Commutation and BLDC Drive

In the BLDC motor, Hall effect sensors are required. The signal is generated by the motor’s Hall effect sensor, and must be decoded in order to determine the right phase-switching sequence [4]. Figure 4 shows the control scheme of the BLDC motor; the reference current I_{ref} is delivered by an outer PI speed controller. Then, the current is controlled using hysteresis controllers.

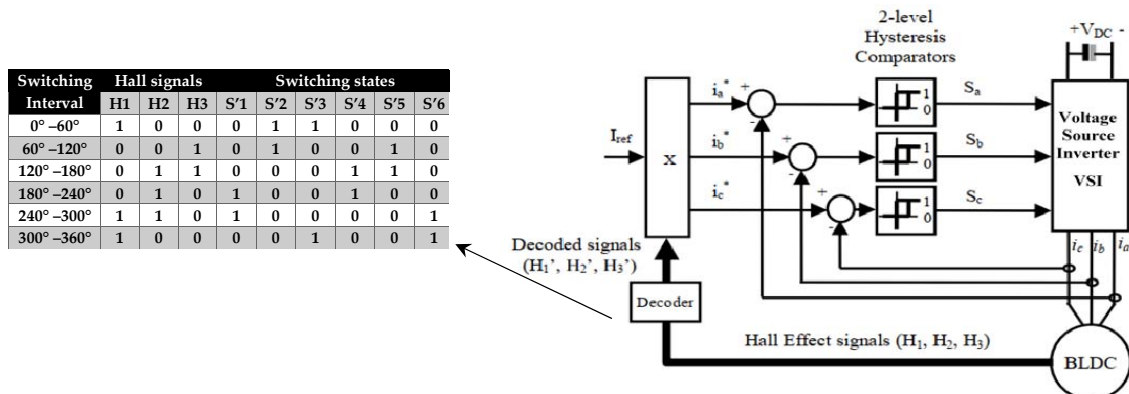


Figure 4. Structure of current control drive for BLDC motor.

4. Partial Shading Effect

Shading in a PV module reduces power, but also creates current mismatch inside a PV series, and string and voltage mismatch between parallel strings. In order to reduce the power damage to the panel, a bypass diode is connected in parallel with the PV module to provide an alternate current channel. A module's cells, on the other hand, no longer carry the same current. As a result, there are numerous maxima on the power–voltage curve. Unfortunately, most standard MPPT algorithms cannot tell the difference between local and global maxima. To investigate the performance of the SWPS under partial shade conditions, the PV modules were adjusted to varied irradiance values (400, 800, and 1000). The P–V characteristic exhibits different maxima, due to the influence of bypass diodes (Figure 5).

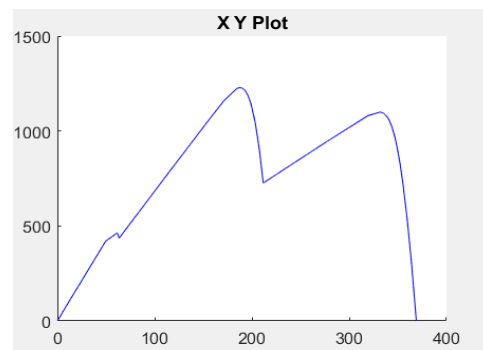


Figure 5. P–V characteristic curves under partial shading.

5. Cuckoo Search Algorithm

5.1. Cuckoo Search Methodology

Firstly, each cuckoo lays one egg at a time and dumps its egg into a randomly chosen nest. Then, the best nest, with high-quality eggs, will carry over to the next generation. The number of available hosts' nests is fixed, and the egg laid by a cuckoo is discovered by the host bird with a probability P_a , such that $0 \leq P_a \leq 1$. In this case, the host bird can either throw the egg away or abandon the nest and build a completely new nest. For simplicity, this last assumption can be approximated by the fraction, P_a , of nests, n , that are replaced by new nests [9].

5.2. Lévy Flight

Lévy flight is a random walk, where step sizes are extracted from Lévy distribution according to the power law $y = l^{-\lambda}$ [10], where l is the flight length and λ is the variance. Since $1 < \lambda < 3$, y has infinite variance. In CS, the nest searching steps of the cuckoo are characterized by Lévy flight. Figure 6 depicts an example of Lévy flight in a 2D plane.

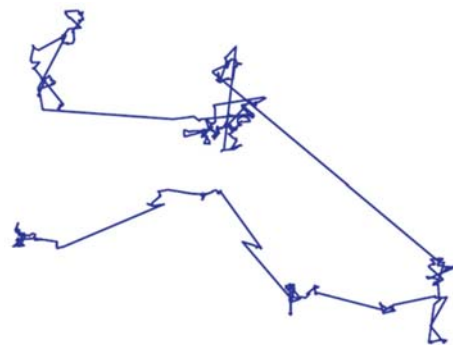


Figure 6. Lévy flight in a 2-dimensional plane.

To generate a new solution, $xt + 1$, for a cuckoo, Lévy flight is performed, as dictated by the following expression [10]:

$$x_i^{(t+1)} = x_i^{(t)} + \alpha \oplus \text{Lévy}(\lambda) \tag{8}$$

where:

\oplus : Entry wise multiplication

λ is the Levy exponent, $x_i^{(t+1)}$ is the new solution, and $x_i^{(t)}$ is the current location (samples/eggs).

$$\text{Lévy}(\lambda) \approx u = l^{-\lambda}, (1 < \lambda < 3) \tag{9}$$

Based on the constraints imposed by the optimization problem, it is important to tune the value of α to obtain the desired step size. In most cases, α is used as follows:

$$\alpha = \alpha_0 (x_j^{(t)} - x_i^{(t)}) \tag{10}$$

where α_0 is the initial step change.

5.3. MPPT for PV Using CS

To use CS for designing MPPT, appropriate variables have to be selected for the search. Firstly, the samples are used, which are the PV voltages in our case, i.e., $V_i (i = 1, 2, \dots, n)$. The total number of samples is defined as n . Then, the step size is denoted by the fitness function J , which is the value of PV power at the MPP. Since J is dependent on the PV voltage, $J = f(V)$. Initially, the generated samples are applied to the PV modules and the power is set as the initial fitness value. The maximum power provided by its corresponding voltage is considered as the current best sample. Thereafter, Lévy flight is performed; consequently, new voltage samples are generated, as follows:

$$V_i^{(t+1)} = V_i^{(t)} + \alpha \oplus \text{Lévy}(\lambda) \tag{11}$$

where $\alpha = \alpha_0 (V_{best} - V_i)$. A simplified scheme of the Lévy distribution is presented as follows:

$$S = \alpha_0 (V_{best} - V_i) \oplus \text{Lévy}(\lambda) \approx K \times \left(\frac{u}{(|v|)^{\frac{1}{\beta}}} \right) (V_{best} - V_i) \tag{12}$$

where k is the Lévy multiplying coefficient. In the following equation, u and v are determined from the normal distribution curves:

$$u = N(0, \sigma_u^2), v = N(0, \sigma_v^2) \tag{13}$$

If Γ denotes the integral gamma function, then the variables σ_u and σ_v are defined as follows:

$$\sigma_u = \left(\frac{\Gamma(1 + \beta) \times \sin(\pi \times \beta/2)}{\Gamma\left(\frac{1+\beta}{2}\right) \times \beta \times (2)^{\left(\frac{\beta-1}{2}\right)}} \right)^{\frac{1}{\beta}}, \sigma_v = 1 \tag{14}$$

The greatest power provided by the voltage is chosen as the new best sample by comparing the power values. Aside from this best sample, the rest are destroyed at random, with a probability of Pa. This procedure mimics the behavior of the host bird finding and then destroying the cuckoo’s eggs. Then, to replace the destroyed samples, new random samples are created. As a result, all the sample powers are measured again, and the current best is chosen by assessing J. The process is repeated until all of the samples have arrived at the MPP.

6. Simulation Results

The proposed SWPS is simulated using MATLAB/Simulink 2018a. A PV array with four solar modules, connected 2×2 in series and in parallel, is considered. In normal conditions, the PV array would be expected to produce 2500 W, with an MPPT voltage and current of 310 V and 8.5 A, respectively, at 1000 W/m^2 solar irradiance and $25 \text{ }^\circ\text{C}$.

The simulation results of the PV side in SWPS, under shaded conditions, using P&O and CS MPPT algorithms, give the resulting waveforms shown in Figures 7 and 8, where “a–b” indicate P&O and “c–d” indicate CS.

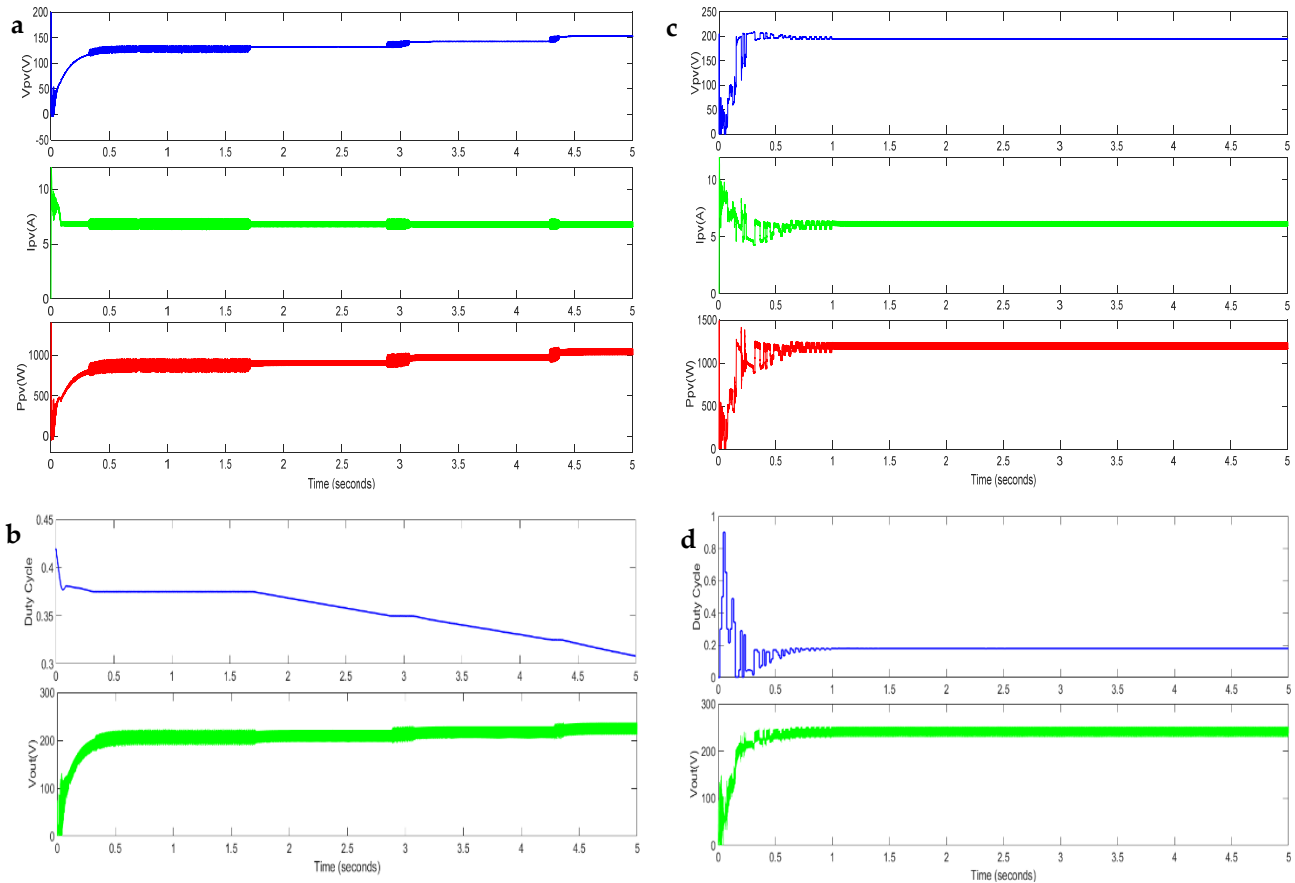


Figure 7. Dynamic performance of the PV generator under shaded conditions using P&O (a,b) and CS (c,d).

As can be observed from the results, the P&O algorithm failed to track the global MPP (Figure 7a,b); it converged to the third peak in Figure 5. The output power from the PV array is reduced. Under partial shading conditions, the output power from the PV array is reduced. On the other hand, the CS method (Figure 7c,d) captured the global peak effectively, avoiding the local maximums, under partial shading conditions, which indicates maximum extraction of the PV power. Compared to P&O, which tracked a local peak, the CS exhibits a faster convergence speed, less oscillation around the MPP under steady-state conditions, and no divergence from the MPP during varying weather conditions. Figure 8 shows the dynamic performance of the BLDC motor under shaded conditions, using P&O and cuckoo search. The BLDC motor shows better performance (i.e., torque and speed) when using the CS algorithm, since it runs on the maximum possible power, as the CS tracks the MPP of the PV array. Table 1 presents the comparison between the two MPPT algorithms, in regards to the power delivered to the pump and the rotor speed.

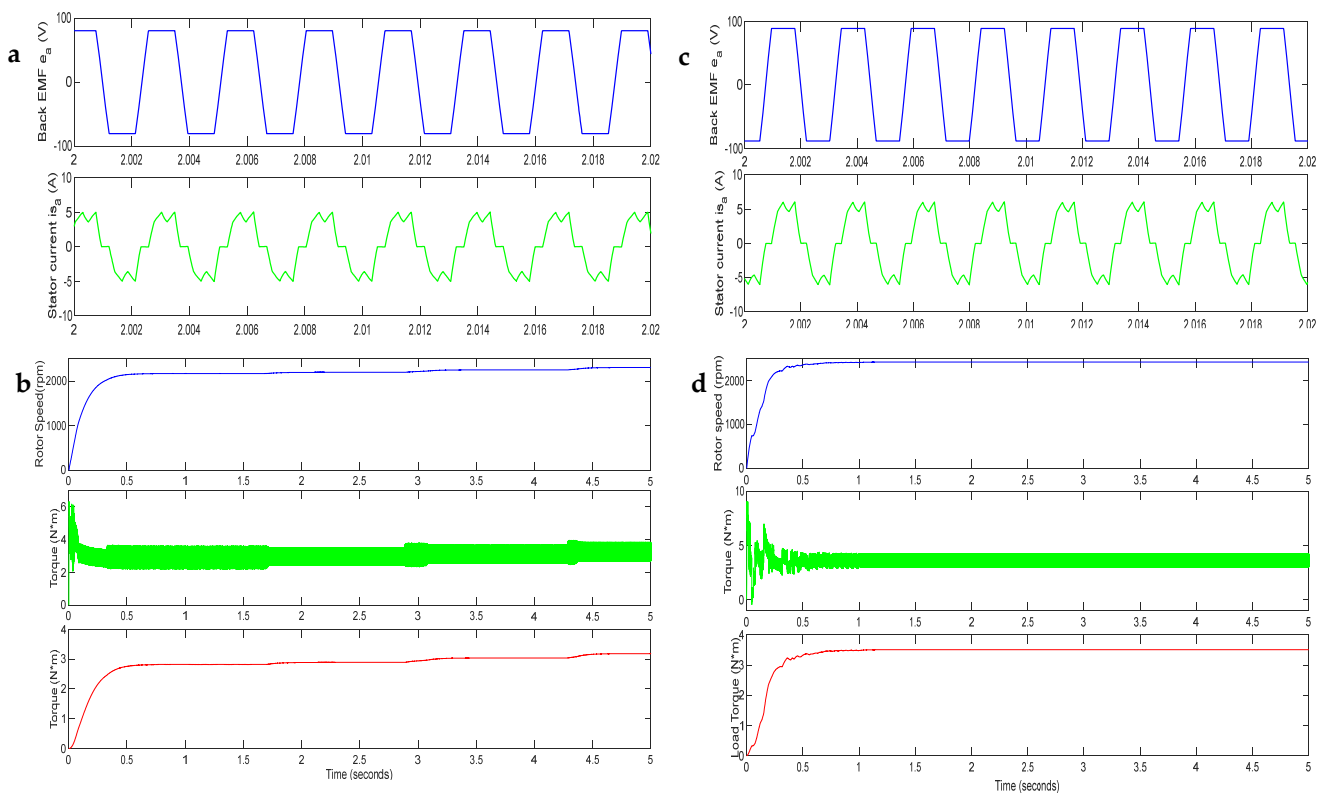


Figure 8. Dynamic performance of the BLDC motor under shaded conditions using P&O (a,b) and CS (c,d).

Table 1. The power and speed values of both MPPT algorithms.

MPPT	Power (W)	Speed (rpm)
P&O	800	2100
Cuckoo Search	1250	2500

7. Conclusions

In this work, a BLDC motor-driven water pumping system, based on PV generation, was designed. The power generated from such systems does not only depend on the climatic conditions, but also highly depends on the applied control technique. MPPT control techniques were used in order to improve the total system efficiency and extract the maximum PV energy under different operating conditions.

The proposed system was simulated and tested using P&O and cuckoo MPPT techniques in MATLAB/Simulink. The performance of the two algorithms was compared under partial shading conditions, where P&O failed to track the global MPP, while the cuckoo search did successfully. Moreover, the results show the improvement in performance of the BLDC motor under non-uniform irradiance conditions.

The parameters of the BLDC motor are as follows:

Rated torque 4.2 N·m, power 1.5 kW, speed 2889 rpm, number of poles 10, phase resistance 0.7 Ω, phase inductance 4 mH, torque constant $K_t = 0.7 \text{ N}\cdot\text{m}/\text{A}$, and moment of inertia 0.0028 kg/m³.

The parameters of the DC–DC converter are as follows:

$C = 2.34 \times 10^{-5} \text{ F}$ and $L = 0.023 \text{ H}$.

Author Contributions: K.H. and M.B. were the major contributors in this work, especially and performing simulation results. A.A. handle writing the manuscript and contributed also in simulation work. A.K. have substantively revised the paper. All authors have read and agreed to the published version of the manuscript.

Institutional Review Board Statement: Not applicable.

Informed Consent Statement: Not applicable.

Data Availability Statement: Not applicable.

Conflicts of Interest: The authors declare no conflict of interest.

Nomenclature

I_{PV} is the cell/module output current (A); I_{ph} is the cell photocurrent (A); I_d is the diode current (A); I_r is the derived current by the shunt resistance (A); I_o is the reverse saturation current of the diode (A); V_{PV} is the cell/module output voltage (V); R and L are BLDC phase resistance and self-inductance; V_a , V_b and V_c are the BLDC terminal phase voltages; i_a , i_b and i_c are the BLDC input currents; e_a , e_b and e_c are the motor back EMF; i is the sample number; t is the number of iterations; $\beta = 1.5$.

References

1. Djeriou, S.; Kheldoun, A.; Mellit, A. Efficiency Improvement in Induction Motor-Driven Solar Water Pumping System Using Golden Section Search Algorithm. *Arab. J. Sci. Eng.* **2018**, *43*, 3199–3211. [[CrossRef](#)]
2. Sontake, V.C.; Kalamkar, V.R. Solar photovoltaic water pumping system—A comprehensive review. *Renew. Sustain. Energy Rev.* **2016**, *59*, 1038–1067. [[CrossRef](#)]
3. Kumar, R.; Singh, B. Single Stage Solar PV Fed Brushless DC Motor Driven Water Pump. *IEEE J. Emerg. Sel. Top. Power Electron.* **2017**, *5*, 1377–1385. [[CrossRef](#)]
4. Kumar, R.; Singh, B. BLDC Motor-Driven Solar PV Array-Fed Water Pumping System Employing Zeta Converter. *IEEE Trans. Ind. Appl.* **2016**, *52*, 2315–2322. [[CrossRef](#)]
5. Talbi, B.; Krim, F.; Rekioua, T.; Laib, A.; Feroura, H. Design and hardware validation of modified P&O algorithm by fuzzy logic approach based on model predictive control for MPPT of PV systems. *J. Renew. Sustain. Energy* **2017**, *9*, 043503. [[CrossRef](#)]
6. Mohapatra, A.; Nayak, B.; Das, P.; Mohanty, K.B. A review on MPPT techniques of PV system under partial shading condition. *Renew. Sustain. Energy Rev.* **2017**, *80*, 854–867. [[CrossRef](#)]
7. Alshareef, M.; Lin, Z.; Ma, M.; Cao, W. Accelerated particle swarm optimization for photovoltaic maximum power point tracking under partial shading conditions. *Energies* **2019**, *12*, 623. [[CrossRef](#)]
8. Yang, X. Suash Deb Cuckoo Search via Lévy flights. In Proceedings of the 2009 World Congress on Nature & Biologically Inspired Computing (NaBIC), Coimbatore, India, 9–11 December 2009; pp. 210–214.
9. Mohamad, A.B.; Zain, A.M.; Nazira Bazin, N.E. Cuckoo Search Algorithm for Optimization Problems—A Literature Review and its Applications. *Appl. Artif. Intell.* **2014**, *28*, 419–448. [[CrossRef](#)]
10. Ahmed, J.; Salam, Z. A Maximum Power Point Tracking (MPPT) for PV system using Cuckoo Search with partial shading capability. *Appl. Energy* **2014**, *119*, 118–130. [[CrossRef](#)]
11. Eltamaly, A.M. An improved cuckoo search algorithm for maximum power point tracking of photovoltaic systems under partial shading conditions. *Energies* **2021**, *14*, 953. [[CrossRef](#)]
12. Malla, S.G.; Bhende, C.N.; Mishra, S. Photovoltaic based water pumping system. In Proceedings of the 2011 International Conference on Energy, Automation and Signal, Bhubaneswar, India, 28–30 December 2011; pp. 1–4.
13. Xiao, W.; Dunford, W.G.; Capel, A. A novel modeling method for photovoltaic cells. In Proceedings of the 2004 IEEE 35th Annual Power Electronics Specialists Conference (IEEE Cat. No.04CH37551), Aachen, Germany, 20–25 June 2004; Volume 3, pp. 1950–1956.
14. Sashidhar, S.; Guru Prasad Reddy, V.; Fernandes, B.G. A Single-Stage Sensorless Control of a PV-Based Bore-Well Submersible BLDC Motor. *IEEE J. Emerg. Sel. Top. Power Electron.* **2019**, *7*, 1173–1180. [[CrossRef](#)]
15. Kamran, M.; Mudassar, M.; Fazal, M.R.; Asghar, M.U.; Bilal, M.; Asghar, R. Implementation of improved Perturb & Observe MPPT technique with confined search space for standalone photovoltaic system. *J. King Saud Univ. Eng. Sci.* **2020**, *32*, 432–441. [[CrossRef](#)]